

## Giant missing row reconstruction of Au on Ge(001)

Arie van Houselt,<sup>1,2</sup> Marinus Fischer,<sup>1,2</sup> Bene Poelsema,<sup>2</sup> and Harold J. W. Zandvliet<sup>1</sup><sup>1</sup>*Physical Aspects of Nanoelectronics, MESA<sup>+</sup> Institute for Nanotechnology, University of Twente, P.O. Box 217, 7500 AE Enschede, The Netherlands*<sup>2</sup>*Solid State Physics, MESA<sup>+</sup> Institute for Nanotechnology, University of Twente, P.O. Box 217, 7500 AE Enschede, The Netherlands*  
(Received 3 September 2008; revised manuscript received 18 November 2008; published 29 December 2008)

We report on a giant missing row reconstruction emerging upon the adsorption and subsequent annealing of (sub)monolayer amounts of Au on Ge(001). The emerging microfacets are of (111) type and reminiscent of those in the well-known  $(2 \times 1)$  missing row reconstruction of the clean (110) surfaces of the fcc transition metals Au, Ir, and Pt. The (111) microfacets are aligned along the  $[110]$  directions and decorated with Au atoms. The periodicity perpendicular to the ridges amounts to 1.6 nm. Surprisingly the corrugation of these Au-induced facets is found to be not less than 0.6 nm. The facets exhibit a  $(\sqrt{3} \times \sqrt{3})R30^\circ$  reconstruction similar to the Au-induced reconstruction of Ge(111). Scanning tunneling microscopy and spectroscopy measurements reveal that the top ridges consist of buckled Ge-dimer rows.

DOI: 10.1103/PhysRevB.78.233410

PACS number(s): 68.43.Fg, 68.37.Ef, 81.16.Rf

Atomic (re)arrangement on surfaces is an important topic for a number of scientific branches ranging from catalysis to solid-state physics. Interatomic distances and surface geometry may dramatically differ from the bulk. Well-known examples of atomic rearrangements at the surface are the (110) surfaces of the noble *5d* metals Au, Pt, and Ir, which exhibit a missing row reconstruction.<sup>1</sup> Every second atom row along the  $[001]$  direction is missing. These surfaces therefore consist of a regular array of (111) microfacets.<sup>2</sup> Here we show similar rearrangements, but on a much larger scale, induced on a Ge(001) surface after deposition of Au and subsequent annealing.

Low-dimensional Au structures have attracted a lot of attention during the last decade. Especially beautiful experiments regarding the formation of atomic Au wires, be it free-standing in vacuum, using break junction techniques,<sup>3</sup> or on surfaces by using scanning tunneling microscopy (STM) have been reported.<sup>4</sup> The tendency to form atomic wires for the *5d* metals Au, Ir, and Pt in break junction experiments has been related to the missing row reconstructions on their (110) surfaces, which resemble atomic chains.<sup>5</sup> Recently the adsorption of Au on Ge(001) has gained interest because of the formation of arrays of nanowires observed by Wang and Altman<sup>6,7</sup> and Schäfer *et al.*<sup>8</sup> Wang and Altman proposed a structural model, in which these nanowires are comprised of symmetric and asymmetric Au-Au dimers aligned perpendicular to the chain direction. The troughs between the wires are proposed to consist of Au-Ge dimers.<sup>6</sup> The observed dimerization is in nice agreement with our observations. Our high-resolution STM results show, however, that the troughs between the nanowires are much deeper, at least 0.6 nm deep. The sides of these grooves are (111) microfacets with an  $(\sqrt{3} \times \sqrt{3})R30^\circ$  Au overlayer reconstruction. The top ridges are comprised of antiferromagnetically ordered buckled dimers running along the  $[110]$  and  $[\bar{1}\bar{1}0]$  directions. Au on Ge(001) behaves differently from Pt on Ge(001), which forms atomic chains on the surface,<sup>9,10</sup> and Pd or Ag on Ge(001), which favors the formation of three-dimensional clusters.<sup>11,12</sup>

The experiments were performed with an Omicron STM

operating in ultrahigh vacuum. Ge(001) substrates were cut from nominally flat 3 in.  $\times$  0.5 mm, about 25  $\Omega$  cm resistance, single-side-polished *n*-type wafers. Samples were mounted on Mo holders and contact of the samples to any other metal during preparation and experiment was carefully avoided. The Ge(001) samples were cleaned by prolonged 800 eV Ar<sup>+</sup> ion sputtering and annealing via resistive heating at 1100( $\pm$ 25) K. The temperature was measured with a pyrometer. After several cleaning cycles the Ge(001) samples were atomically clean and exhibited a well-ordered  $(2 \times 1)/c(4 \times 2)$  domain pattern.<sup>13</sup> Subsequently, an equivalent of 0.20–0.30 monolayers of Au was deposited onto the surface at room temperature. Au was evaporated by resistively heating a W wire wrapped with high-purity Au (99.995%). After Au deposition the sample was annealed at 650( $\pm$ 25) K and then cooled down to room temperature by radiation quenching before placing it into the STM for observation.

Figure 1 shows room-temperature STM images after deposition of Au on Ge(001) and subsequent annealing. The images show “nanostripes” which are separated 1.6 nm apart. They run along the  $[110]$  directions of the Ge(001) crystal. Their height as determined from Fig. 1 is at least 0.6 nm, i.e., four times higher than a single step on Ge(001). Comparable heights are measured for positive bias voltages. Consequently, these structures are far too high to be explained by atomic chains on a substrate as in the case of Pt on Ge(001).<sup>9,10</sup> In cases that the surface contains such small protruding structures, it might easily be that the structures on the surface are actually sharper than the apex of the STM tip. The obtained STM image will, as a result, contain ghost images of the tip as well. Such a tip artifact can be seen in Figs. 1(b) and 1(d), in which an additional minitip at the side of the STM tip apex is present.

We propose that the nanostripes are microfacets of Ge. Based on the alignment of the stripes along the  $[110]$  directions we consider the  $(11n)$  facets of Ge as possible candidates. From the 0.6 nm surface corrugation we deduce that they should be (111) facets because it is impossible to form facets with such a height using higher index planes. We presume therefore that the Au-induced nanostripes are alternat-

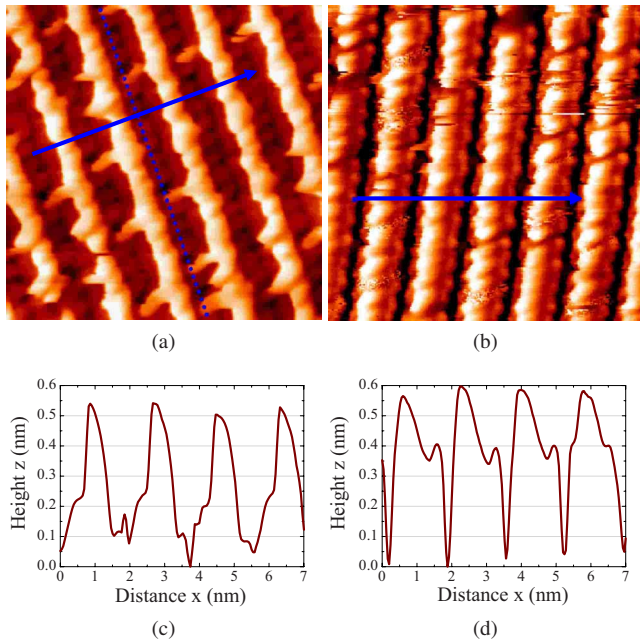


FIG. 1. (Color online) STM images obtained after deposition of Au on Ge(001). Images sizes are  $10.0 \times 10.0 \text{ nm}^2$ , tunneling current is 3 nA,  $T=300 \text{ K}$ , and sample biases are  $-1.0$  and  $-0.9 \text{ V}$  in, respectively, (a) and (b). Height line profiles along the solid blue arrows are plotted in (c) and (d). Note the tip artifacts in (b) and (d).

ing  $(\bar{1}\bar{1}\bar{1})$  and  $(\bar{1}\bar{1}\bar{1})$  facets, leading to a giant missing row reconstruction.

The behavior of Au on Ge(111) is well studied by surface x-ray diffraction<sup>14</sup> and STM.<sup>15</sup> Deposition of Au on Ge(111) leads to a  $(\sqrt{3} \times \sqrt{3})R30^\circ$  Au overlayer structure. Howes *et al.*<sup>14</sup> performed a detailed x-ray diffraction study to determine the geometry of this structure. They describe the Au/Ge(111) surface as a “missing top layer” structure, in which half of the Ge atoms in the top bilayer of the bulk-terminated Ge(111) lattice has been removed, leaving a single layer to which the Au atoms can bond (see Fig. 2). The dangling Ge bonds are passivated by Au trimers.

Based on this knowledge and our STM data, we propose a model for the Au-induced nanostripes. The model is shown in Fig. 3. We start with a bulk-truncated structure of the facets with a 1.6 nm separation of the facets. Guided by the Au/Ge(111) results, half of the Ge atoms from the top bilayer on the facet sides are replaced by Au atoms, leading to a  $(\sqrt{3} \times \sqrt{3})R30^\circ$  reconstruction. Based on our STM images we believe that the top ridges are comprised of antiferromagnetically buckled Ge dimer rows, which resemble the buckled Ge dimer rows on a bare Ge(001) surface very well. The ridges are six atomic layers high, i.e., 0.84 nm.

Figure 4(a) shows an STM image of the Au-induced facets. The top ridges are clearly dimerized and the distance between neighboring dimers is exactly 0.4 nm. Occasionally one finds missing dimer defects in the top ridge. The similarities with the regular buckled Ge dimer rows of the clean Ge(001) surface are striking. The dimers in the top ridges buckle in an antiferromagnetic order. An antiphase boundary in this antiferromagnetic order shows up as a single noisy dimer similar to the noisy dimers in the Ge(001) surface near

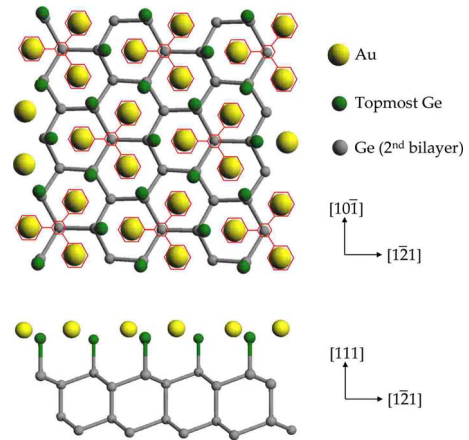


FIG. 2. (Color online) Schematic representation (top view and side view) of the  $(\sqrt{3} \times \sqrt{3})R30^\circ$  Au overlayer structure on Ge(111). Au trimers are embedded in the topmost Ge(111) plane. As a guide for the eyes it is indicated which Au atoms form a Au trimer. Half of the Ge atoms of the topmost layer are removed by the incorporation of Au atoms in the lattice. Atomic positions are drawn to scale.

missing dimer defects.<sup>16</sup> At the antiphase boundary the dimers cannot decide whether to align with its left or right neighbor.  $I(t)$  measurements at a fixed height over such noisy dimers reveal that these dimers are flip flopping. A time trace of the tunneling current and a histogram of the residence

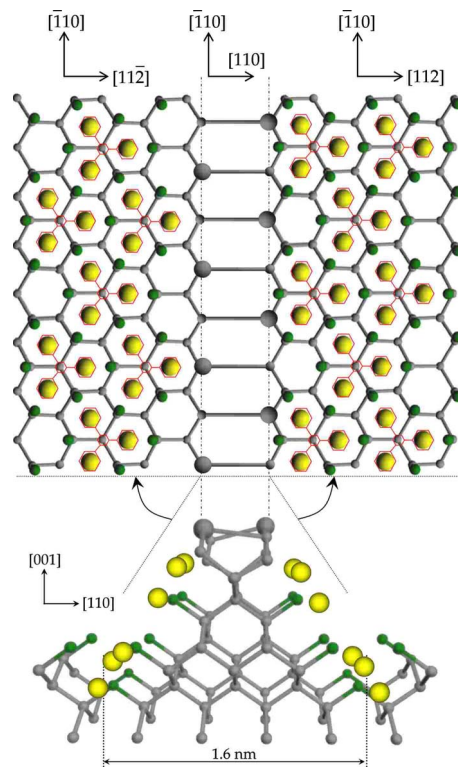


FIG. 3. (Color online) Schematic “exploded” top view and side view of the  $(\bar{1}\bar{1}\bar{1})$  and  $(\bar{1}\bar{1}\bar{1})$  facets. The green Ge atoms are the topmost Ge atoms in the  $(\sqrt{3} \times \sqrt{3})R30^\circ$  Au overlayer. Note that the Ge dimers on top are buckled (the larger atoms are the higher atoms of the dimers).

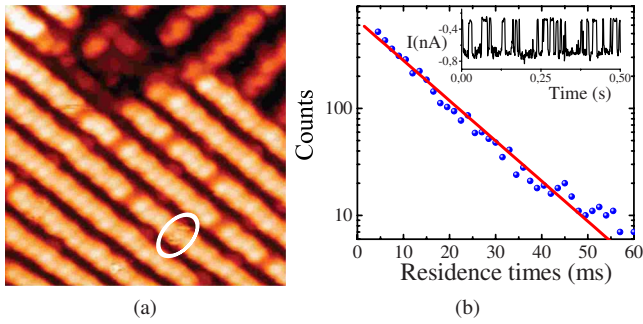


FIG. 4. (Color online) (a) STM image ( $10.0 \times 10.0 \text{ nm}^2$ , sample bias of  $-1.0 \text{ V}$ , and tunneling current of  $0.6 \text{ nA}$ ) of the Au-induced facets. The top ridges resemble the zigzag dimer rows on Ge(001). At antiphase boundaries in the antiferromagnetic dimer ordering, the dimers appear noisy (see white ellipse). (b) Histogram of the residence times above a noisy appearing dimer. The blue line is the theoretical fit for a random process (Poisson distribution). The sampling rate was  $666.7 \text{ Hz}$ . The inset shows an  $I(t)$  trace measured over the flip-flopping dimer marked by the white ellipse in (a).

times in the two configuration of a noisy dimer extracted from many time traces are shown in Fig. 4(b). The histogram reveals that we are dealing with a stochastic process.<sup>16</sup>

In addition, we have also performed scanning tunneling spectroscopy on the top ridges of the Au-induced facets. Figure 5(a) shows the spatially averaged local density of states ( $dI/dV)/(I/V)$  averaged over the facet top ridges in Fig. 4(a). The local density of state (LDOS) of  $c(4 \times 2)$  and reconstructions on Ge(001) are shown in Fig. 5(b) for comparison. The peaks in these curves are extensively discussed in Ref 17. The peaks at  $-1.0$  and  $0.8 \text{ eV}$  are assigned to the  $\sigma$  and  $\sigma^*$  bonds of the dimer, respectively, while the peaks at  $-0.8$ ,  $-0.5$ , and  $0.5 \text{ eV}$  are attributed to the dangling bonds of the dimer. The strong agreement of the LDOS measured on the top of the facet ridges and the LDOS measured on the clean Ge(001) surface strongly suggests that the top of the facet ridges consists of Ge dimers rather than Au atoms or dimers. The LDOS of the Au-induced nanofacets agrees surprisingly well with the LDOS of the  $c(4 \times 2)$ -reconstructed Ge(001). The latter is fully in line with the observed zigzag pattern in Fig. 4(a).

Figure 6(a) shows an STM image acquired with an accidentally present asymmetric tip apex. This type of measure-

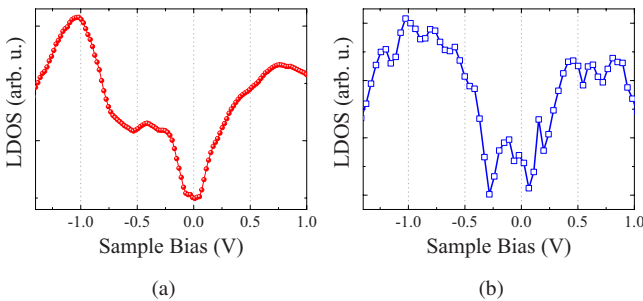


FIG. 5. (Color online) (a) Spatially averaged LDOS ( $dI/dV)/(I/V)$  averaged over the top ridges of the facets in Fig. 4(a). (b) Spatially averaged LDOS recorded on the  $c(4 \times 2)$  reconstruction on Ge(001).

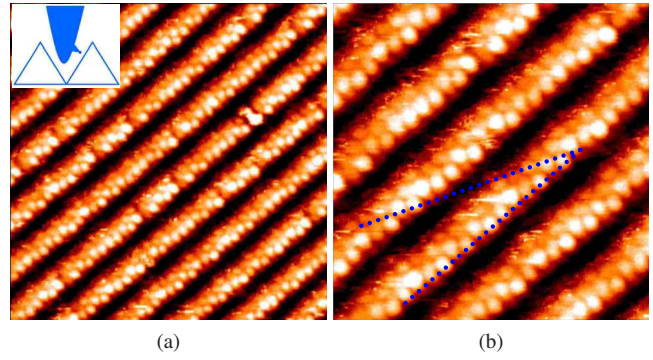


FIG. 6. (Color online) (a) STM image ( $12.5 \times 12.5 \text{ nm}^2$ , sample bias of  $-0.6 \text{ V}$ , tunneling current of  $0.8 \text{ nA}$ ) recorded with an asymmetric tip apex. The inset shows a schematic representation of the measurement with an asymmetric tip apex. Note that the Au trimers show up as a single protrusion. (b) STM image ( $7.4 \times 7.4 \text{ nm}^2$ , sample bias of  $-0.6 \text{ V}$ , and tunneling current of  $0.8 \text{ nA}$ ) recorded with the same tip. The angle between the dotted blue lines is  $22.5^\circ \pm 2^\circ$ .

ments with an asymmetric tip allows one to image one of the facets. The other facet side of the groove appears featureless. At the nicely imaged side, Au trimers are visible as single white protrusions. The ordering of the protrusions is in perfect agreement with the model depicted in Fig. 3. Figure 6(b) shows a smaller scale image acquired with the same tip. Two dotted blue lines are drawn: one along the  $[1\bar{1}0]$  direction (along the facet ridge) and the other along the densely packed Au trimer direction. The measured angle between these lines is  $22.5^\circ \pm 2^\circ$ , in perfect agreement with the model presented in Fig. 3. [Note that the angle of  $30^\circ$  on the (111) facets should be projected onto the 001 plane.]

In Figs. 1(a) and 4(a) one can observe a strong corrugation in the troughs between the facets. From time to time also bridges between the facets are visible. A line profile along the blue line in Fig. 1(a) is shown in Fig. 7. It shows the corrugation in the troughs. The image is recorded again with a very sharp but slightly asymmetric tip apex. The corrugation in between the facets in Fig. 1(a) is therefore contributed to the lowest Au trimers in the trough. The Au trimers show up single protrusions in the troughs. The distance between

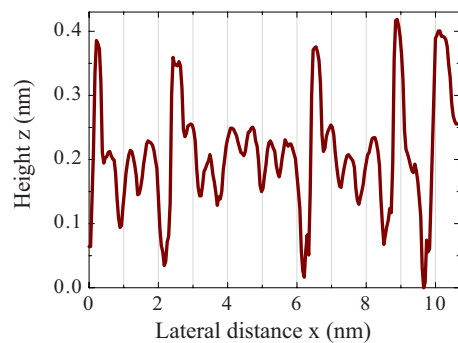


FIG. 7. (Color online) Height profile along the dotted blue line in Fig. 1(a). Note that the bridges are positioned exactly at locations where an antiphase boundary in the  $(\sqrt{3} \times \sqrt{3})R30^\circ$  Au overlayer occurs (compare Fig. 3).

the trimers is 0.6 nm. The bridges are positioned exactly at locations where an antiphase boundary in the  $(\sqrt{3} \times \sqrt{3})R30^\circ$  Au overlayer occurs (compare Fig. 3). At one side of the bridge the distance to the neighboring Au trimer is shorter, namely, 0.4 nm (here always at the right of the bridges in Fig. 7). At the other side the distance to the neighboring Au trimer is longer, namely, 0.8 nm.

Finally, the driving force for the development of these Au-induced structures must be an overall reduction in the surface free energy. The surface free energy of the Au-decorated (111) facets should, hence, be lower than the surface free energy of the bare Ge(001) surface per unit area divided by  $\sqrt{3}$ .

In summary, the deposition of Au on Ge(001) leads to the

development of a well-ordered pattern of (111) faceted nanogrooves. The constituting (111) facets are decorated with Au atoms into a  $(\sqrt{3} \times \sqrt{3})R30^\circ$  pattern. Scanning tunneling spectroscopy measurements reveal that the top of the ridges are comprised of buckled Ge-dimer rows, which are ordered in an antiferromagnetic fashion. Antiphase boundaries in the buckling registry show up as dynamically flip-flopping dimers.

*Note added in proof.* Recently, we became aware of the work by Schäfer *et al.* on the Au/Ge(001) system.<sup>8</sup>

This work was financially supported by the Stichting voor Fundamenteel Onderzoek der Materie (FOM) (Contract No. 03PR2208).

- 
- <sup>1</sup>R. Koch, M. Borbonus, O. Haase, and K. H. Rieder, Appl. Phys. A **55**, 417 (1992).
- <sup>2</sup>J. J. Schulz, M. Sturmat, and R. Koch, Phys. Rev. B **62**, 15402 (2000).
- <sup>3</sup>A. I. Yanson, G. R. Bollinger, H. E. van den Brom, N. Agraït, and J. M. van Ruitenbeek, Nature (London) **395**, 783 (1998).
- <sup>4</sup>N. Nilus, T. M. Wallis, and W. Ho, Science **297**, 1853 (2002).
- <sup>5</sup>R. H. M. Smit, C. Untiedt, A. I. Yanson, and J. M. van Ruitenbeek, Phys. Rev. Lett. **87**, 266102 (2001).
- <sup>6</sup>J. Wang, M. Li, and E. I. Altman, Phys. Rev. B **70**, 233312 (2004).
- <sup>7</sup>J. Wang, M. Li, and E. I. Altman, Surf. Sci. **596**, 126 (2005).
- <sup>8</sup>J. Schäfer, C. Blumenstein, and S. Meyer, Phys. Rev. Lett. **101**, 236802 (2008).
- <sup>9</sup>O. Gurlu, O. A. O. Adam, H. J. W. Zandvliet, and B. Poelsema, Appl. Phys. Lett. **83**, 4610 (2003).
- <sup>10</sup>M. Fischer, A. van Houselt, D. Kockmann, B. Poelsema, and H. J. W. Zandvliet, Phys. Rev. B **76**, 245429 (2007).
- <sup>11</sup>J. Wang, M. Li, and E. I. Altman, J. Appl. Phys. **100**, 113501 (2006).
- <sup>12</sup>L. H. Chan and E. I. Altman, Phys. Rev. B **66**, 155339 (2002).
- <sup>13</sup>H. J. W. Zandvliet, Phys. Rep. **388**, 1 (2003).
- <sup>14</sup>P. B. Howes, C. Norris, M. S. Finney, E. Vlieg, and R. G. van Silfhout, Phys. Rev. B **48**, 1632 (1993).
- <sup>15</sup>L. Seehofer and R. L. Johnson, Surf. Sci. **318**, 21 (1994).
- <sup>16</sup>A. van Houselt, R. van Gastel, B. Poelsema, and H. J. W. Zandvliet, Phys. Rev. Lett. **97**, 266104 (2006).
- <sup>17</sup>O. Gurlu, H. J. W. Zandvliet, and B. Poelsema, Phys. Rev. Lett. **93**, 066101 (2004).